First principles study of small palladium cluster growth and isomerization

ARTICLE *in* INTERNATIONAL JOURNAL OF QUANTUM CHEMISTRY · JUNE 2007

Impact Factor: 1.43 · DOI: 10.1002/qua.21315

First Principles Study of Small Palladium Cluster Growth and Isomerization

CHEN LUO,[1] CHENGGANG ZHOU,[1,2] JINPING WU,[1] T. J. DHILIP KUMAR,[2] NADUVALATH BALAKRISHNAN,[2] ROBERT C. FORREY,[3] HANSONG CHENG[4]

[1]*Institute of Theoretical Chemistry and Computational Materials Science, China University of Geosciences, Wuhan, People's Republic of China 430074*

[2]*Department of Chemistry, University of Nevada at Las Vegas, Las Vegas, NE 89154*

[3]*Department of Physics, Penn State University, Berks-Lehigh Valley College, Reading, PA 19610-6009*

[4]*Air Products and Chemicals, Inc., 7201 Hamilton Boulevard, Allentown, PA 18195-1501*

Received 12 December 2006; accepted 10 January 2007
Published online 20 February 2007 in Wiley InterScience (www.interscience.wiley.com).
DOI 10.1002/qua.21315

ABSTRACT: Structures and physical properties of small palladium clusters Pd_n up to $n = 15$ and several selected larger clusters were studied using density functional theory under the generalized gradient approximation. It was found that small Pd_n clusters begin to grow 3-dimensionally at $n = 4$ and evolve into symmetric geometric configurations, such as icosahedral and *fcc*-like, near $n = 15$. Several isomers with nearly degenerate average binding energies were found to coexist and the physical properties of these clusters were calculated. For several selected isomers, relatively moderate energy barriers for structural interchange for a given cluster size were found, implying that isomerization could readily occur under ambient conditions. © 2007 Wiley Periodicals, Inc. Int J Quantum Chem 107: 1632–1641, 2007

Key words: Pd clusters; cluster evolution; cluster isomerization

Introduction

Transition metal (TM) clusters have been a subject of active theoretical and experimental studies in the recent decades [1–9]. At the most fundamental level, evolution of structure and physicochemical properties from small TM clusters to bulk metals has been one of the central issues in condensed matter physics research. Technologically, TM clusters serve as catalysts in many industrially important chemical processes. They are also used extensively in semiconductor and sensing devices, magnetic storage materials, and constitute important components of nanomaterials for various applications [10–18]. TM clusters exhibit a wide variety of geometries, isomers, and sizes. Many studies

Correspondence to: H. Cheng; e-mail: chengh@airproducts.com
Contract grant sponsor: Research Foundation for Outstanding Young Teachers, China.
Contract grant sponsor: University of Geosciences, Wuhan.
Contract grant number: CUGQNL0519.
Contract grant sponsor: US Department of Energy.
Contract grant number: DE-FG36–05GO85028.

have shown that the physicochemical properties of these clusters are critically dependent on these structural arrangements. Understanding of the structural and property evolution of TM clusters is essential for design and development of novel materials and processes for a broad area of applications. Of particular interest are the palladium clusters, since they serve as excellent catalysts in many heterogeneous catalytic systems. These clusters exhibit some unique physicochemical properties [12–15, 19], which have been the subject of intense theoretical and experimental studies [3, 4, 13, 20–29]. They show an unique magnetic property and promise for potential application on supported metal catalysts. The properties of these clusters are determined by their electronic structures and, ultimately, by the cluster structural arrangements.

Like other TM clusters, palladium clusters exhibit numerous isomers for a given size and the structures of these clusters have been extensively reported in literature. Several theoretical calculations have shown that many of these isomers possess similar binding energies, suggesting that they may coexist under certain experimental conditions. One interesting question concerning the relative stability of these isomers thus arises: under what conditions would one isomer evolve into another? One of the objectives of the present study is to address this issue. Understanding of the isomer structural exchange is important to gain insight into the catalytic reactivity of palladium clusters. As palladium clusters grow, the transition of palladium clusters from atomic to bulk metallic behavior may be monitored by photoemission spectroscopy [30]. In this study, we study Pd_n cluster structures and growth using density functional theory (DFT). Our main focus is to explore the cluster growth pathways, understand the transition from small clusters to the bulk structure, quantify the energetics of isomeric structural exchange and, ultimately, gain insight into the chemical properties of palladium catalysts. We discovered several Pd_n cluster structures that have not been previously reported. These new cluster structures are energetically favorable with higher or comparable binding energies than the previously reported cluster structures of the same size. These findings allow us to gain detailed insight into the cluster structural evolution and the energetics for isomeric structural exchange.

Computational Method

The present study utilized DFT under the generalized gradient approximation (GGA) with Pedrew–Wang's exchange-correlation functional (PW91) as implemented in DMol package [31–35]. Spin-polarization scheme was employed to deal with the electronically open-shell system. The spin states and the magnetic moments were then determined based on the calculated energies of spin-up and spin-down orbitals. To describe the valence electrons, we employed a double numerical basis set augmented with polarization functions, and the core electrons are described with an effective core potential (ECP), which also accounts for the relativistic effect expected to be significant for heavy elements in the periodic table. Electronic structure calculations for systems containing TMs are known to be notoriously difficult to converge. This is particularly the case for TM clusters due to the large number of *d*-electrons involved. To enhance the SCF convergence, we initially used a small value of thermal smearing (~0.001Ha) to obtain structures close to the equilibria and then sequentially removed the value until it reaches to zero. This guarantees that the number of unpaired electrons is an integer. All cluster geometries were fully optimized without imposing symmetry constraints, except for the icosahedral structures for which point group symmetries were utilized to simplify the calculations. For a given cluster size, a variety of initial structures were selected followed by energy minimization, yielding numerous stable isomers. The cluster structural search scheme used in our calculations is to add a new atom on the preceding cluster with the highest binding energy at various possible binding sites and then to identify the energetically most stable site via geometry optimization. To avoid missing structures with more favorable binding energies, additional caution was taken by placing the new addition to the preceding clusters with energies close to the highest binding energy cluster followed by energy minimization.

The average cluster binding energy was calculated using the following expression:

$$\Delta E_n = [n\,E(\mathrm{Pd}) - E(\mathrm{Pd}_n)]/n, \quad (n = 2, 3, \ldots), \quad (1)$$

where $E(\mathrm{Pd})$ represents the atomic energy of Pd and $E(\mathrm{Pd}_n)$ is the energy of Pd_n cluster. Subsequently, we evaluated the cluster ionization poten-

tial (IP), electron affinity (EA) and magnetic moment (μ) defined by

$$\mathrm{IP}_n = E(\mathrm{Pd}_n^+) - E(\mathrm{Pd}_n), \quad (2a)$$

$$EA_n = E(\mathrm{Pd}_n^-) - E(\mathrm{Pd}_n), \quad (2b)$$

$$\mu = (m_u - m_d)/2, \quad (2c)$$

where m_u and m_d are the numbers of spin-up and spin-down electrons with $m_u \geq m_d$, respectively.

For comparison purpose, we also performed calculations to evaluate the cohesive energy, which is identical to the average bulk binding energy in the present case. This was done by imposing a periodic boundary condition in the DFT calculation using the primitive unit cell of palladium. The Brillioun zone integration was performed with $8 \times 8 \times 8$ *k*-points using the Monkhorst and Pack scheme. Both atomic coordinates and cell parameters were fully relaxed upon structural optimization, yielding the cell parameters within ± 0.01 Å of the experimental crystal structure.

Results and Discussions

For a given size of cluster, full structure optimization usually yields numerous isomers. Figure 1 displays the main isomeric structures obtained for Pd_n (n = 2–15). The corresponding average binding energies are shown underneath. A cluster with the highest binding energy at a given size is placed at the front. The highest binding energy structures for n = 2–10 have been reported previously [2, 3, 10, 11], and our optimized geometries are in good agreement with other DFT calculations. To the best of our knowledge, the highest average binding energy structures for n = 11–15 are reported for the first time in this work.

The calculated average binding energy of palladium dimer is 0.692 eV, while the experimental value varies from 0.37 to 0.57 eV [36, 37], respectively, slightly lower than the calculated one. The calculated bond length of 2.555 Å is also slightly longer than the experimental value of 2.48 Å [38]. Other reported theoretical calculations gave the dimer bond distance of 2.52 Å [3] in close agreement with what is reported here. Pd_3 is an isosceles triangle, slightly distorted from the equilateral triangle due to the Jahn–Teller effect. For the same reason, Pd_4 with the highest binding energy is a slightly distorted tetrahedron. From Pd_4 to Pd_7, the clusters grow with bipyramid configurations with increasing average bond distances and binding energies. A previous study using the DFT-based tight-binding model [39] predicted that the planar Pd_7-c is the most stable structure. However, our calculation suggests that the planar geometry is considerably less stable than the bipyramid configuration. From Pd_8, deviation from the symmetric bipyramid structure occurs and the cluster growth appears to be quite "irregular". Nevertheless, the difference of the calculated average binding energies among the isomers is rather small, which suggests that these isomers may coexist thermodynamically. For Pd_9, Karabacak et al. [3, 4] predicted that $Pd_{9\text{-e}}$ structure is the most stable configuration using molecular dynamics and slow-quenching technique with an embedded-atom potential. Our DFT calculation predicts that this is the least stable structure and the configuration with distorted double octahedrons fused with one facet is the most stable one. It is worth noting that $Pd_{9\text{-d}}$ can be regarded as a half icosahedron configuration with an average binding energy 0.037 eV lower than that of $Pd_{9\text{-a}}$.

From Pd_{10}, certain characteristics of icosahedral geometry appear in most of our calculations. For Pd_{10}, the highest average binding energy occurs for a structure that is similar to a half icosahedral configuration. Calculations by Futschek et al. [2] using PAW coupled with plane-wave basis set as implemented in the VASP package suggests that $Pd_{10\text{-d}}$ is the most stable cluster. Our study shows that the average binding energy of $Pd_{10\text{-d}}$ is only slightly lower than that of $Pd_{10\text{-a.}}$

For Pd_{11}, the highest binding energy structure $Pd_{11\text{-a}}$ is constructed by three octahedrons, each of which fuses one facet with the other two. The average bond length of $Pd_{11\text{-a}}$ is less than that of the other isomers, indicating that this structure is the most close-packed. $Pd_{11\text{-e}}$ was previously predicted as the most stable structure [2]. Our calculations suggest that the average binding energies of the n = 11 isomers are close to each other but the close-packed structure $Pd_{11\text{-a}}$ is energetically most favorable.

For the Pd_{12}, the highest binding energy structure $Pd_{12\text{-a}}$ is composed of two octahedrons and a pentagonal bipyramid and has the shortest average bond length, indicating an essentially close-packed structure. $Pd_{12\text{-b}}$ is an icosahedral structure with a vacant center. This structure was predicted to be unstable and will relax to a centered icosahedron with a defect in the outer shell [2]. We found that it

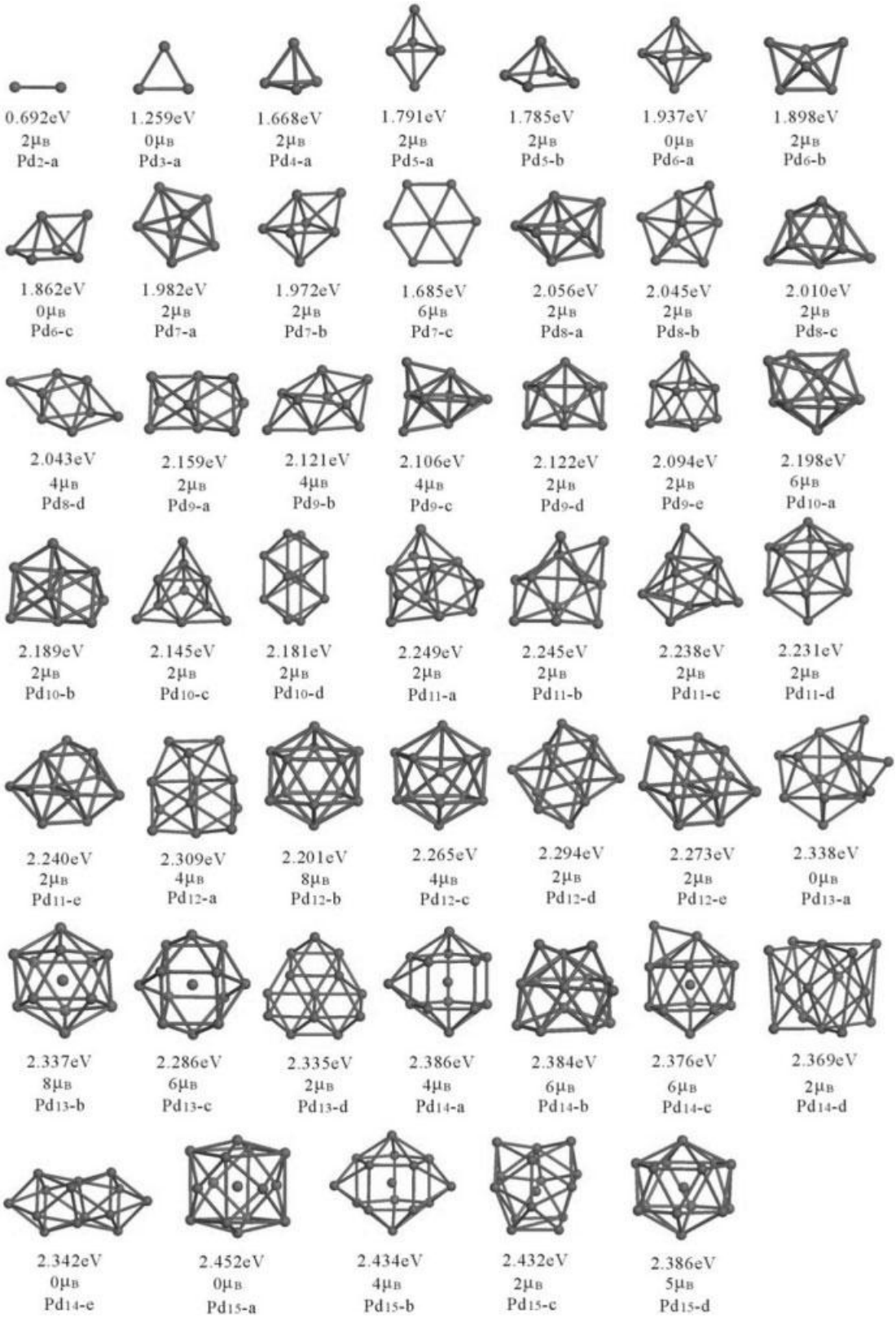

FIGURE 1. The main optimized isomeric structures of Pd_n (n = 2–15). The average binding energy per Pd atom is shown underneath.

could still stabilize without significant deformation but its average binding energy is considerably lower than that of $Pd_{12\text{-}a}$ by 0.108 eV. Separately, $Pd_{12\text{-}c}$ [3] and $Pd_{12\text{-}e}$ [2] were also predicted as the most stable structure. Their average binding energies are slightly lower than that of $Pd_{12\text{-}a}$. We note that $Pd_{12\text{-}c}$ can be viewed as a distorted icosahedron.

For Pd_{13}, the highest binding energy structure $Pd_{13\text{-}a}$ is built upon $Pd_{10\text{-}a}$ by adding three capped atoms on the triangular facets. $Pd_{13\text{-}b}$ is a typical centered icosahedral structure with an average binding energy of 2.337 eV, nearly degenerated with that of $Pd_{13\text{-}a}$. The icosahedral geometry was predicted to be the most stable structure in previous calculations [3, 10, 11, 14, 40]. $Pd_{13\text{-}c}$ is a centered cube with four capped atoms on its side facets. $Pd_{13\text{-}d}$ was also predicted to be the most stable structure [2]. Our calculation shows that the difference of average binding energies between $Pd_{13\text{-}a}$ and $Pd_{13\text{-}d}$ is only 0.003 eV.

For Pd_{14}, the highest average binding energy structure $Pd_{14\text{-}a}$ takes a pentagon prismatic configuration with three capped atoms. The close-packed $Pd_{14\text{-}b}$ is formed by adding three atoms on three triangular facets of $Pd_{11\text{-}d}$. $Pd_{14\text{-}c}$ is a typical icosahedron by adding one atom on a trigonal facet. $Pd_{14\text{-}d}$ is close to a *fcc*-like cluster with slight distortion. The geometric configuration of $Pd_{14\text{-}e}$ is somewhat similar to the icosahedral structure of Pd_{19} (see Fig. 1) with the main difference being that the rings are formed by five atoms in $Pd_{19\text{-}ic}$ instead of four atoms here. The difference in the calculated average binding energies among the isomers is very small. We note in particular that all three geometric configurations, close-packed, *fcc*-like, and icosahedron, coexist for $n = 14$.

For $n = 15$, the highest average binding energy cluster, $Pd_{15\text{-}a}$, is a typical *fcc*-like structure with the atoms in the faces slightly out of plane. The average bond length of $Pd_{15\text{-}a}$ is also much shorter than the other isomers, indicating a close-packed structure. The fact that $Pd_{15\text{-}a}$ is energetically most stable suggests that *fcc*-like growth may start dominating the cluster evolution at a small size. Adding one atom on two different square side facets of $Pd_{14\text{-}b}$ respectively yields the structures, $Pd_{15\text{-}b}$ and $Pd_{15\text{-}c}$ with nearly identical average binding energies. The structure of $Pd_{15\text{-}d}$ is somewhat similar to that of $Pd_{13\text{-}b}$ except the five-membered rings in $Pd_{13\text{-}b}$ are replaced by six-membered rings in $Pd_{15\text{-}d}$.

Figure 2 displays the calculated bondlength distributions of the highest average binding energy clusters. The majority of the bonds in the clusters fall into the range of 2.6–2.8 Å. The sharp increase from Pd_3 to Pd_4 results from the first structural transition from two dimensions to three dimensions. The bondlength increases slowly as the cluster size increases until $n = 8$ at which cluster grows in a rather "irregular" fashion. However, the general trend is that clusters preferably adopt geometric configurations that are most close packed. As a consequence, the bondlengths for $n \geq 8$ remain more or less constant.

The energetic and topological similarity of the close-packed, icosahedral, and *fcc*-like structures observed in small palladium clusters suggests that structural transitions from the close-packed configurations to icosahedral and, ultimately, to the bulk-like *fcc* configurations could occur at a relatively small cluster size. To gain insight into the evolution, we performed calculations on four selected icosahedral structures for $n = 13$, 19, 25 and 55 and four selected *fcc*-like structures for $n = 14$, 23, 32 and 38. The optimized structures as well as the calculated average binding energies are shown in Figure 3. The choice of *fcc*-like structures is somewhat arbitrary but it helps us to gain at least a qualitative understanding of the cluster growth pathway.

Figure 4 displays the average binding energy of the highest average binding energy clusters together with the selected icosahedral and *fcc*-like clusters verses the inverse of cluster size. For $1/n \rightarrow 0$, the average binding energy approaches to the bulk cohesive energy. Several interesting features can be readily observed:

1. The average binding energy of small palladium clusters increases with the cluster size;
2. At around $n = 13$, the average binding energies of both icosahedral and *fcc*-like structures are comparable to that of the close packed "irregular" clusters, indicating that the transition from the "irregular" structure to the icosahedral and *fcc*-like structures could occur at a small cluster size;
3. In the approximate range of $20 \leq n \leq 50$, the icosahedral and *fcc*-like structures coexist but after that the icosahedral structures appear to dominate the cluster growth. Unfortunately, due to the computational intensity, we are unable to optimize the energy for large clusters using the DFT method. Therefore, it is difficult to find out at what size of a cluster

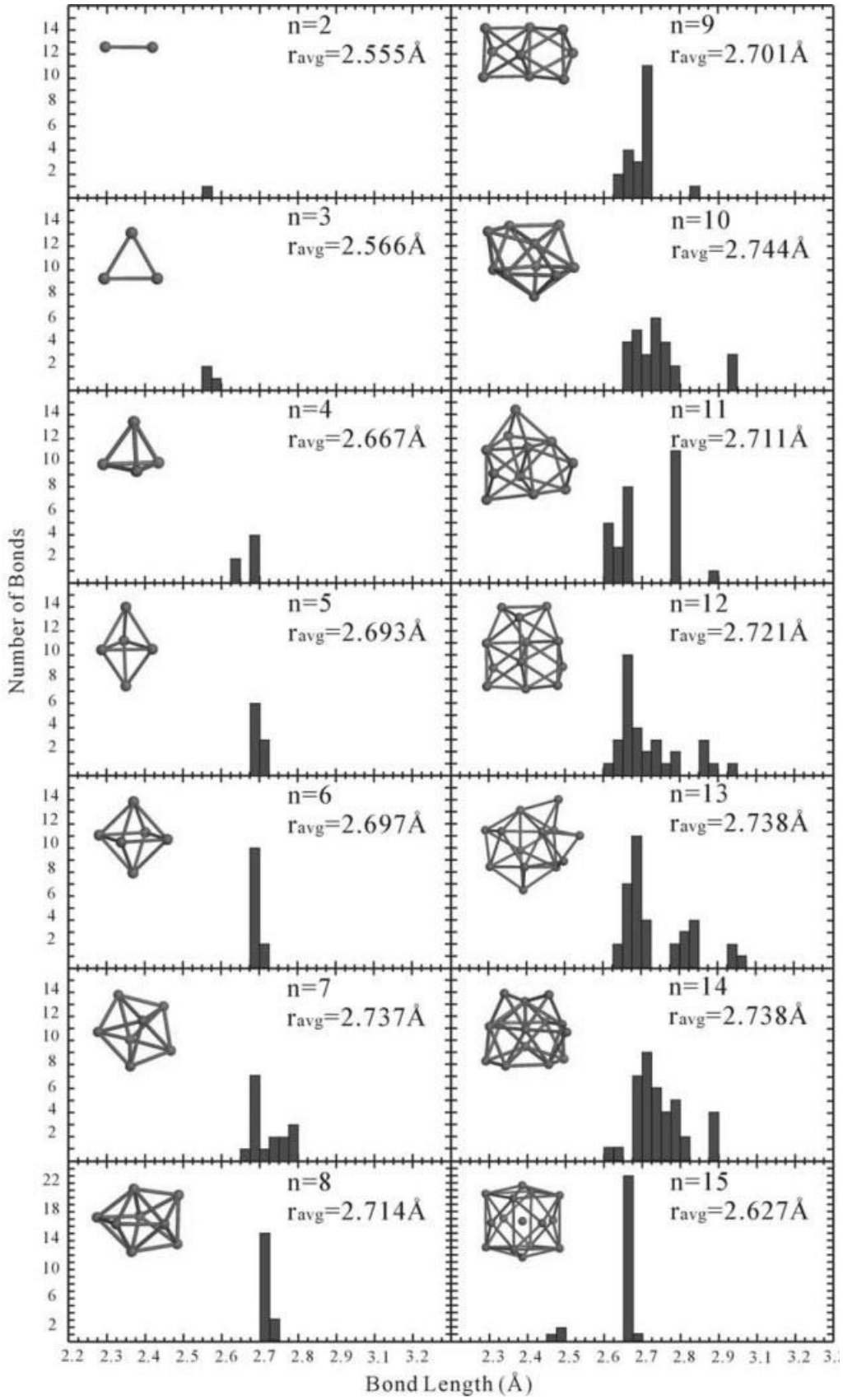

FIGURE 2. The calculated bondlength distribution of the highest average binding energy clusters.

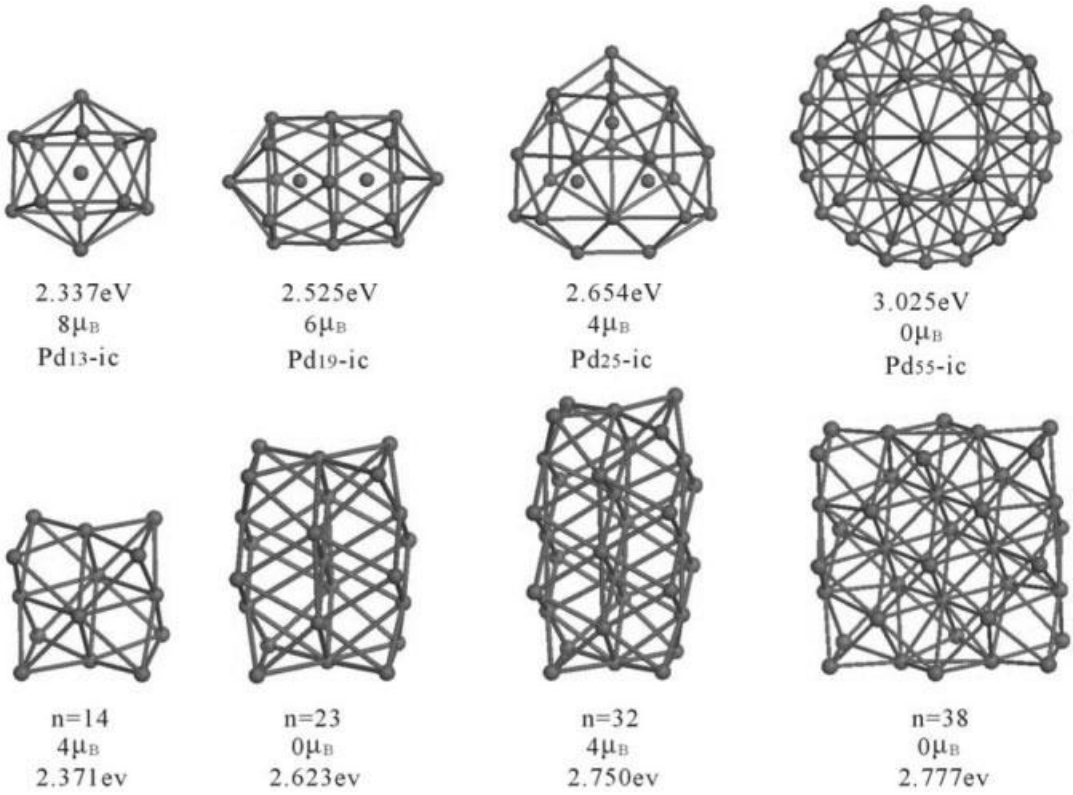

FIGURE 3. Selected icosahedral structures for $n = 13$, 19, 25, and 55 and *fcc*-like structures for $n = 14$, 23, 32, and 38. All structures were fully optimized with the average binding energies underneath.

transition from icosahedral geometry to the bulk structure occurs.

We note that Karabacak et al. [3] obtained a highest average binding energy structure for Pd_{19}.

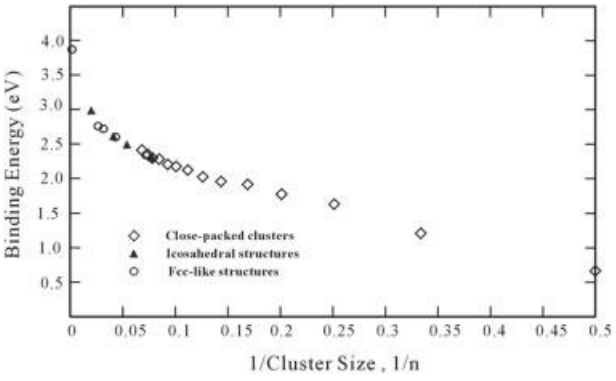

FIGURE 4. The average binding energy of the highest average binding energy clusters and the selected icosahedral and *fcc*-like clusters verses the inverse of cluster size.

Upon energy minimization of their structure, we obtained a structure of Pd_{19} that is energetically and topologically similar to the icosahedral configuration. It is also worth noting that the structural transition of small palladium cluster differs significantly from that of platinum [9] and copper [6–8]. For platinum clusters, a structural transition from triangular clusters to icosahedral clusters occurs at the cluster size approximately $n = 19$ and a less energetically favorable transition from triangular clusters to *fcc*-like clusters takes place around $n = 38$. For copper clusters, it was found that structural transitions from the triangular growth clusters to the icosahedral and *fcc*-like clusters occur at approximately $n = 16$ and $n = 32$, respectively.

Results presented in Figure 1 suggest many isomers of palladium clusters exhibit nearly degenerate average binding energies and thus these isomers could coexist from thermodynamic point of view. An interesting question is how easy these isomers could transform from one structure to another or, in other words, whether the structural exchange of the isomers is kinetically feasible. It is

computationally very difficult to calculate the structural exchange pathways, which could be numerous, and rigorous studies on the kinetics require calculations on the transition states along these paths. To gain qualitative or semi-quantitative insight into the feasibility of isomer structural exchange, we selected a few isomers of various cluster sizes to study the transformation between isomers along the pathway defined by linear synchronous transit (LST) using the structures of the isomers using the following equation:

$$\boldsymbol{r}_i = \sigma\, \boldsymbol{r}_i^{(1)} + (1 - \sigma)\boldsymbol{r}_i^{(2)}, \quad (0 \le \sigma \le 1), \qquad (3)$$

where r_i, $r_i^{(1)}$, and $r_i^{(2)}$ are the coordinates of the ith atom along the LST pathway and of isomers (1) and (2), respectively, and $i = 1, \ldots, N$ (N is the number of atoms of the isomers). Single point energy calculations were then performed along the LST pathway. The structures and energetics so calculated of course do not necessarily represent the minimum energy path. However, they do represent a possible transformation path with an energy barrier higher than that of the minimum energy pathway. Therefore, the calculated activation energy can serve as the upper bound of the true energy barrier of the minimum energy pathway.

We selected five pairs of isomers from Figure 1, $Pd_{6\text{-}a}/Pd_{6\text{-}b}$, $Pd_{9\text{-}b}/Pd_{9\text{-}c}$, $Pd_{13\text{-}b}/Pd_{13\text{-}c}$, $Pd_{15\text{-}a}/Pd_{15\text{-}b}$, and $Pd_{15\text{-}b}/Pd_{15\text{-}d}$, and calculated their LST pathways. The results are shown in Figure 5. The coordinate correlations between isomers were carefully considered so that the atom pairs would reside in similar positions upon transformation. Nevertheless, it can be readily seen from Figure 5 that structures of some of the isomer pairs selected in the present study are radically different. However, the calculated energy barriers for the selected LST pathways are considerably moderate in most cases, suggesting that structural isomerization could readily take place at or near ambient temperature. Figure 5 also indicates that the isomerization barrier increases with cluster size as expected. It can be envisaged that for large clusters, isomerization will become increasingly difficult. However, we speculate that localized structural rearrangements could still occur without too much energy penalty.

Figure 6 displays the calculated total magnetic moments of the highest average binding energy clusters for $n = 2$–15. Earlier experiments suggested that small palladium clusters are nonmagnetic [41–43], while photoelectron spectra suggested that Pd_n

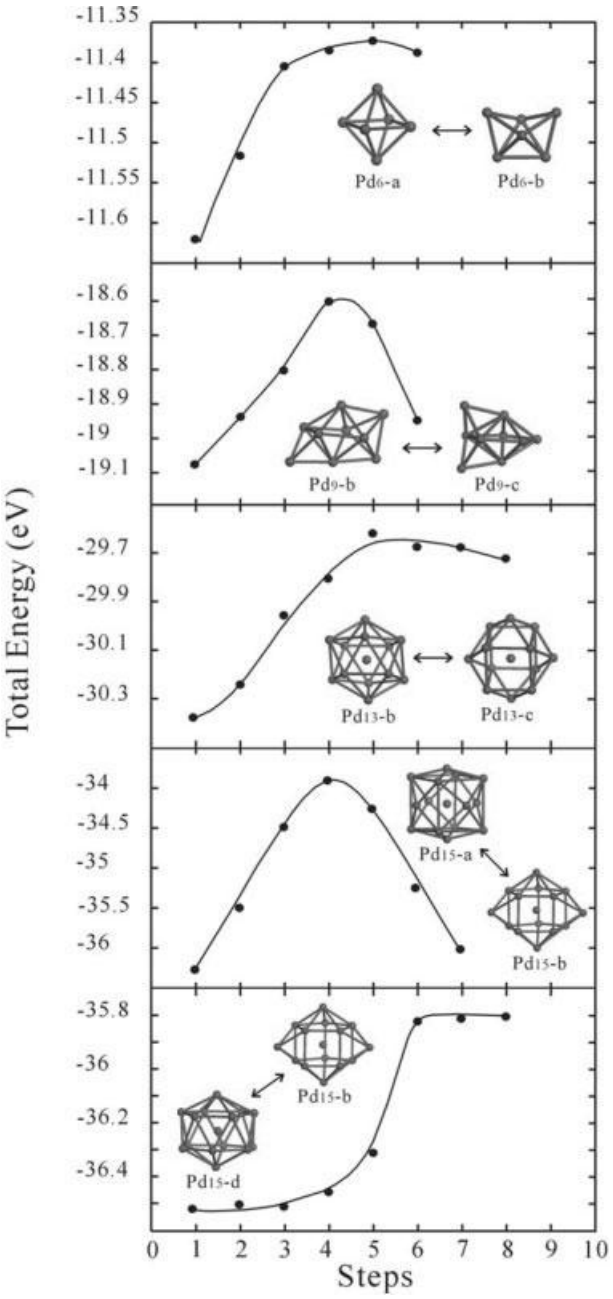

FIGURE 5. Cluster isomerization energy of the selected pairs of isomers along the LST pathway.

($n < 7$) clusters have Ni-like spin distribution [44] and predicted that $n = 8$ is the critical size for magnetic–nonmagnetic transition [44, 45]. The present study suggests that the cluster magnetism varies with cluster size and shape. Isomers with nearly degenerate binding energies may differ significantly in their magnetic moments. For example, for the close-packed structure, $Pd_{13\text{-}a}$, our calculation yields no

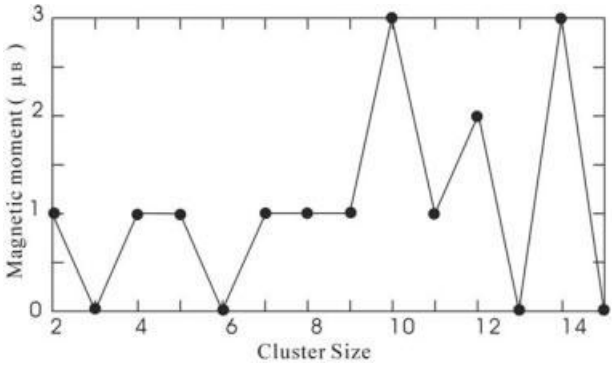

FIGURE 6. The calculated total magnetic moments of the highest average binding energy clusters for n = 2–15.

magnetism, while for the icosahedral structure, $Pd_{13\text{-}b}$, which is nearly degenerate with $Pd_{13\text{-}a}$ in terms of average binding energy, the calculated total magnetic moment is $4\mu_B$/atom. This result agrees well with the studies by Reddy et al., [46, 47] who also found that 13-atom clusters of 3d and 4d TMs adopting an icosahedral symmetry have nonzero magnetic moments. Therefore, depending on specific experimental conditions, under which specific structures of cluster isomers are produced, the measured magnetic moments could be very different. Our calculated cluster magnetism is essentially consistent with what were reported by T. Futschek et al., [2], Kumar et al. [48] and Barreteau et al. [39] for similar cluster structures. The calculated IP and EA are shown in Figure 7(a) and (b), respectively. The results show that the calculated IPs decrease rapidly with cluster size from $n = 2$ to $n = 5$ and then become steady as the size of clusters increases. The calculated EAs generally increase with cluster size. We note that the EA values of Pd_3 and Pd_7 obtained from experiments [49–51] are substantially higher than our results. The underestimation of cluster EAs largely stems from fact that the basis set used in the present computational method does not include diffuse functions, which are known to be essential for accurate electronic structure calculations of anionic species.

Conclusions

We have performed extensive theoretical studies on small palladium clusters using DFT. Computational search for energy minima on cluster potential energy surfaces yielded numerous isomers at a given cluster size, which is an important feature shared by many TM clusters. In particular, we found many of these isomers are nearly degenerate in energy despite the fact that their topological structures differ considerably, indicating that these isomers could coexist thermodynamically. Kinetically, the estimated energy barriers of transforming structures from one isomer to another were rather moderate, suggesting that these isomers may readily exchange their structures at ambient conditions. The barrier increases with cluster size and thus the larger is the cluster the more stable the isomer structure will be. Nevertheless, we speculate that localized structural arrangement in a large palladium cluster could occur in view of the relatively small energy barriers for small isomer structural exchange.

In the present study, we focused mostly on three structural patterns of palladium clusters: the close-packed "irregular" structures, the icosahedral structures and *fcc*-like structures. It was found even at a small size of the clusters ($n \geq 13$), the isomers of these structural patterns are nearly degenerate. Unfortunately, the wide structural variety of large clusters and the associated heavy computational cost prohibit us to perform DFT calculations to study structural transitions at a large cluster size. Nevertheless, we expect that the icosahedral structural pattern would dominate the cluster growth as the size of clusters increases.

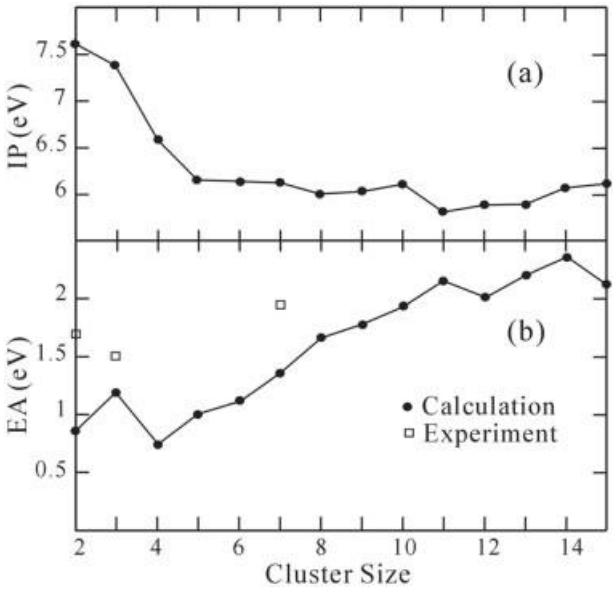

FIGURE 7. The calculated cluster ionization potential (IP) (a) and electron affinity (EA) (b).

One of the driving forces to study palladium clusters is to understand their catalytic properties. Understanding the cluster structures and energetics is the first step toward understanding the structure–activity relationships in many catalytic processes. We are currently studying the role of small palladium clusters in catalyzing dissociative chemisorption of molecular hydrogen and the results will be reported in due course.

References

1. Cheng, H.; Wang, L. S. Phys Rev Lett 1996, 77, 51.
2. Futschek, T.; Marsman, M.; Hafner, J. J Phys Condens Matter 2005, 58, 532.
3. Karabacak, M.; Özçelik, S.; Güvenç, Z. B. Surf Sci 2002, 507–510, 636.
4. Karabacak, M.; Özçelik, S.; Güvenç, Z. B. Surf Sci 2003, 532–535, 306.
5. Guo, X.-Y. Phys Chim Sin 2003, 19, 174.
6. Guvelioglu, G. H.; Ma, P.; He, X.; R. C., Forrey, Cheng, H. Phys Rev Lett 2005, 94, 026103.
7. Guvelioglu, G. H.; Ma, P.; He, X.; R. C., Forrey, Cheng, H. Phys Rev B 2006, 73, 155436.
8. Forrey, R. C.; Guvelioglu, G. H.; Ma, P.; He, X.; Cheng, H. Phys Rev B 2006, 73, 155437.
9. Nie, A.; Wu, J.; Zhou, C.; Yao, S.; Luo, C.; Forrey, R. C.; Cheng, H. Int J Quan Chem (in press).
10. Cui, O.; Musaev, D. G.; Morokuma, K. J. J Chem Phys 1998, 108, 8418.
11. Efremenko, I.; Sheintuch, M. J Mol Catal A: Chem 2000, 160, 445.
12. Kumar, V. Comput Mater Sci 2006, 35, 375.
13. Aguilera-Granja, F.; Montejano-Carrizales, J. M.; Berlanga-Ramirez, E. O.; Vega, A. Phys Rev B 1998, 58, 1665.
14. Watari, N.; Ohnishi, S. Phys Rev B 1998, 58, 1665.
15. Che, M.; Bennett, C. O. Adv Catal 1989, 36, 55.
16. Xiao, Y.; Yu, G.; Yuan, J.; Wang, J.; Chen, Z. Electrochim Acta 2006, 51, 4218.
17. Walter, E. C.; Murray, B. J.; Favier, F.; Kaltenpoth, G.; Penner, R. M. J Phys Chem B 2002, 106, 11407.
18. Walter, E. C.; Favier, F.; Penner, R. M. Anal Chem 2002, 74, 1546.
19. Stanislsus, S. A.; Cooper, B. H. Catal Rev Sci Eng 1994, 36, 75.
20. Nava, P.; Sierka, M.; Ahlrichs, R. Phys Chem Chem Phys 1999, 74, 405.
21. Aguilerea-Granja, F.; Momtejano-Carrizales, J. M.; Verlanga-Ramirez, E. O.; Vega, A. Phys Lett B 2004, 354, 271.
22. Aguilerea-Granja, F.; Momtejano-Carrizales, J. M.; Vega, A. Phys Lett A 2004, 332, 107.
23. Aguilerea-Granja, F.; Momtejano-Carrizales, J. M.; Vega, A. Solid State Commun 2005, 133, 573.
24. Giordano, L.; Pacchioni, G. Surf Sci 2005, 575, 197.
25. Reifsnyder, S. N.; Otten, M. M.; Lamn, H. H. Catal Today 1998, 39, 317.
26. Takeguchi, M.; Mitsuishi, K.; Tanaka, M.; Furuya, K. Surf Sci 2003, 532–535, 671.
27. Chang, Z.; Thornton, G. Surf Sci 2000, 459, 303.
28. Koyasu, K.; Naono, Y.; Akutsu, M.; Mitsui, M.; Nakajima, A. Chem Phys Lett 2006, 442, 62.
29. Hu, H. N.; Chen, H. Y.; Yu, S. Y.; Chen, L. J.; Chen, J. L.; Wu, G. H. J Magn Magn Mater 2006, 299, 170.
30. Colbert, J.; Zangwill, A.; Strongin, M. Phys Rev B 1983, 27, 1378.
31. Perdew, J. P.; Wang, Y. Phys Rev B 1992, 45, 13244.
32. Delley, B. J Chem Phys 1990, 92, 508.
33. Delley, B. J Phys Chem 1996, 100, 6107.
34. Delley, B. Int J Quan Chem 1998, 69, 423.
35. Delley, B. J Phys Chem 1996, 113, 7756.
36. Lin, S.; Straus, B.; Kant, A. J Chem Phys 1969, 51, 2282.
37. Lide, D. R., Ed. Handbook of Chemistry and Physics; CRC Press: Boca Raton, FL, 1995.
38. Herzberg, G. Mol Spec Mol Struct 1979, 4.
39. Barretau, C.; Guirado-López, R.; Spanjaard, D.; Desjonqúeres, M. S.; Oles, A. Phys Rev B 2000, 61, 7781.
40. Rey, C.; Gallego, L. J.; García-Rodeja, J.; Alonso, J. A.; Iñiguez, M. P. Phys Rev B 1993, 48, 8253.
41. Cox, A. J.; Louderback, J. G.; Bloomfield, L. A. Phys Rev Lett 1993, 71, 923.
42. Cox, A. J.; Louderback, J. G.; Apsel, S. E.; Bloomfield, L. A. Phys Rev B 1994, 49, 12295.
43. Douglass, D. C.; Bucher, J. P.; Bloomfield, L. A. Phys Rev B 1992, 45, 6341.
44. Canteför, G.; Everhardt, W. Phys Rev Lett 1996, 76, 4975.
45. Zhao, J. J.; Chen, X. S.; Sun, Q.; Liu, F.; Wang, G. H. Europhys Lett 1995, 32, 113.
46. Dunlap, B. I. Phys Rev A 1990, 41, 5691.
47. Reddy, B. V.; Khanna, S. N.; Dunlap, B. I. Phys Rev Lett 1993, 70, 3323.
48. Kumar, V.; Kawazoe, Y. Phys Rev B 2002, 66, 144413.
49. Pontius, N.; Bechthold, P. S.; Eberhardt, M. N. J Elec Spectrosc Relat Phenom 2000, 106, 107.
50. Ervin, K. M.; Ho, J.; Lineberger, E. C. J Chem Phys 1998, 89, 4514.
51. Ho, J.; Polak, M. L.; Ervin, K. M.; Lineberger, W. C. J Chem Phys 1993, 99, 8542.